

Introduction

With passive seismic interferometry we can retrieve the earth's reflection response by cross-correlation of ambient-noise recordings (Draganov et al., 2009). One of the major assumptions underpinning this concept is that the noise sources are uniformly distributed throughout the subsurface, which is often not the case in practise. To overcome this problem, Wapenaar et al. (2008) suggested replacing cross-correlation by multi-dimensional deconvolution. The implementation of their idea requires separation of the passive incident wavefields from their free-surface-related multiples through time-gating. For this reason, applications have been limited to transient sources with a distinct incident arrival. An alternative is to introduce the incident wavefields of the passive sources as additional unknowns in the inversion process, as suggested by van Groenestijn and Verschuur (2009). Here we take a different, but practical, approach by showing that time-gating can be implemented after cross-correlation but before inversion. This idea opens the way for applying multi-dimensional deconvolution to simultaneously acting noise sources.

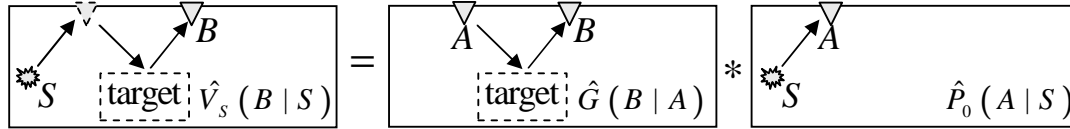


Figure 1: Illustration of the forward model for passive seismic interferometry by multi-dimensional deconvolution; S denotes a subsurface source location, whereas A and B are receivers.

Theory

The underlying forward model is shown in Figure 1. The incidence pressure field \hat{P}_0 at receiver A is convolved (in the frequency domain this is multiplication) with the unknown Green's function $\hat{G}(B|A)$ (between virtual source A and receiver B) to produce the scattered particle velocity field \hat{V}_s in B (Wapenaar et al., 2008):

$$\hat{V}_s(B|S) = \int \hat{G}(B|A) \hat{P}_0(A|S) d^2A, \quad (1)$$

where S is the source location and the integral is over the virtual-source coordinates A . Seismic interferometry by multi-dimensional deconvolution is accomplished by inverting equation 1 for \hat{G} , given \hat{P}_0 and \hat{V}_s . \hat{P}_0 can be estimated from the time-gated incident particle velocity field \hat{V}_0 through $\hat{P}_0 \approx (\rho c / \cos \phi) \hat{V}_0$, where ρ is the density, c the wave velocity and ϕ the propagation angle with respect to the surface. To achieve independence from subsurface source information, we assume that $\cos \phi \approx 1$ (meaning near-normal incidence) such that $\hat{P}_0 \approx \hat{V}_0$, where a scaling factor ρc is omitted for convenience. Least-squares inversion of equation 1 under substitution of $\hat{P}_0 \approx \hat{V}_0$ is equivalent to solving the following normal equation (Menke, 1989):

$$\int \hat{V}_s(B|S) \hat{V}_0^*(A'|S) d^2S \approx \int \hat{G}(B|A) \left[\int \hat{V}_0(A|S) \hat{V}_0^*(A'|S) d^2S \right] d^2A. \quad (2)$$

We discretize equation 2 in terms of monochromatic matrices $\hat{\mathbf{V}}_0$, $\hat{\mathbf{V}}_s$ and $\hat{\mathbf{G}}$ (representing \hat{V}_0 , \hat{V}_s and \hat{G} , respectively) where the columns host (real or virtual) sources and the rows host receivers (Berkhout, 1982). The equation can now be solved with a stabilization parameter ε for regularization:

$$\hat{\mathbf{G}} \approx \hat{\mathbf{V}}_s \hat{\mathbf{V}}_0^\dagger \left[\hat{\mathbf{V}}_0 \hat{\mathbf{V}}_0^\dagger + \varepsilon^2 \mathbf{I} \right]^{-1}, \quad (3)$$

where superscript \dagger denotes the complex conjugate transpose. Implementation of equation 3 requires separation of incident and scattered wavefields for each individual subsurface source, which poses a major limitation. Assume that the incidence field cannot be separated from the total field $\hat{\mathbf{V}} = \hat{\mathbf{V}}_s + \hat{\mathbf{V}}_0$. However, we can still compute

$$\hat{\mathbf{V}} \hat{\mathbf{V}}^\dagger = \hat{\mathbf{V}}_0 \hat{\mathbf{V}}_0^\dagger + \left[\hat{\mathbf{V}}_s \hat{\mathbf{V}}_0^\dagger + \hat{\mathbf{V}}_0 \hat{\mathbf{V}}_s^\dagger \right] + \hat{\mathbf{V}}_s \hat{\mathbf{V}}_s^\dagger. \quad (4)$$

The first term in equation 4 will have its major contribution close to $|t|=0$. The term between the square brackets will have its dominant contributions at $|t| > t_1$, where t_1 is the two-way travel-time of the first reflector. If this reflector is located sufficiently deep, we can separate the first term in equation 4 from the term between the square brackets by time-gating after cross-correlation. The last term $\hat{\mathbf{V}}_s \hat{\mathbf{V}}_s^\dagger$ is relatively weak and could be neglected. Wapenaar and Fokkema (2006) show how an integral over transient sources can be replaced by an ensemble average over simultaneously acting noise sources. We apply similar logic to equation 2 to show that

$$\langle \hat{V}_s(B) \hat{V}_0^*(A') \rangle \approx \int \hat{G}(B|A) \left[\langle \hat{V}_0(A) \hat{V}_0^*(A') \rangle \right] d^2 A. \quad (5)$$

$\hat{V}_0(A)$ and $\hat{V}_s(B)$ are the incident field in A and the scattered field in B from simultaneously acting noise sources and $\langle \cdot \rangle$ is an ensemble average. $\langle \hat{V}_0(A) \hat{V}_0^*(A') \rangle$ and $\langle \hat{V}_s(A) \hat{V}_0^*(A') \rangle$ can be estimated from $\langle \hat{V}(A) \hat{V}^*(A') \rangle$ by time-gating after cross-correlation. If we compute these cross-correlations over sufficient receiver locations A , equation 5 can be inverted, yielding an estimate of the unknown Green's function $\hat{G}(B|A)$. This method can compensate for anisotropic illumination by simultaneously acting passive noise sources, as we will show with an example.

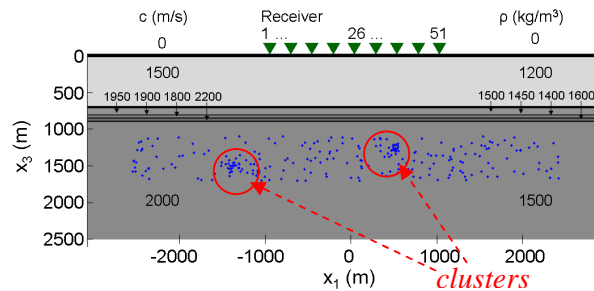


Figure 2: Configuration for the passive example; receivers are indicated by green triangles, sources by blue dots; in red we indicate the presence of two source clusters.

Example

The configuration for the passive example is shown in Figure 2. 51 vertical-component receivers are located at the earth's surface every 40 m. 200 passive sources are located in the subsurface with an irregular distribution with average spacing of 25 m; additionally, two source clusters are superimposed (with 20 and 30 sources, respectively). In Figures 3a-3c we show the individual components of the $\hat{\mathbf{V}}\hat{\mathbf{V}}^\dagger$ -correlation at receiver 26. In Figure 4a we show their superposition. A representation of the $\hat{\mathbf{V}}_0\hat{\mathbf{V}}_0^\dagger$ - and $\hat{\mathbf{V}}_s\hat{\mathbf{V}}_0^\dagger$ -response (Figures 3a and 3b) can be easily obtained from the $\hat{\mathbf{V}}\hat{\mathbf{V}}^\dagger$ -gather (Figure 4a) by isolating all events $|t| < 0.5s$ and $t > 0.5s$, respectively. The $\hat{\mathbf{V}}_s\hat{\mathbf{V}}_s^\dagger$ -response (Figure 3c) is indeed weak and can be neglected. In Figure 4b we compare a slice of the retrieved reflection response by cross-correlation (followed by time-gating), with a reference response that is computed with an active source at the virtual source location. The retrieval is imperfect due to the presence of the noise-source clusters. In Figure 4c we see the result after multi-dimensional deconvolution. Note that the imprint of the noise clusters has been compensated. Next we repeat the procedure, but with simultaneously acting noise sources. In Figure 5a we show a slice of the ensemble average $\langle \hat{v}(A)\hat{v}^*(A') \rangle$. Compared to the transient sources (Figure 4a), the cross-correlated wavelet signature seems slightly different and the record is noisier. However, the same spatial imprint of the source clusters can be observed. We can separate $\langle \hat{v}_0(A)\hat{v}_0^*(A') \rangle$ and $\langle \hat{v}_s(A)\hat{v}_0^*(A') \rangle$ by isolating all events $|t| < 0.5s$ and $t > 0.5s$, respectively. With this procedure we can retrieve the reflection response either through cross-correlation (Figure 5b) or multi-dimensional deconvolution (Figure 5c). Note that the latter has largely removed the imprint of the noise-source clusters at the cost of some inversion artefacts due to the noisy character of the data.

Conclusion

The reflection response as retrieved by cross-correlation of ambient-noise recordings is blurred by an imprint of the subsurface source distribution. This imprint can be found in the retrieved response cluttered around $t=0$ in the cross-correlation panels. We showed that if the first reflection is sufficiently deep, the imprint could be isolated by time-gating after cross-correlation and used for multi-dimensional deconvolution. We showed that this procedure can correct for anisotropic illumination of subsurface noise sources.

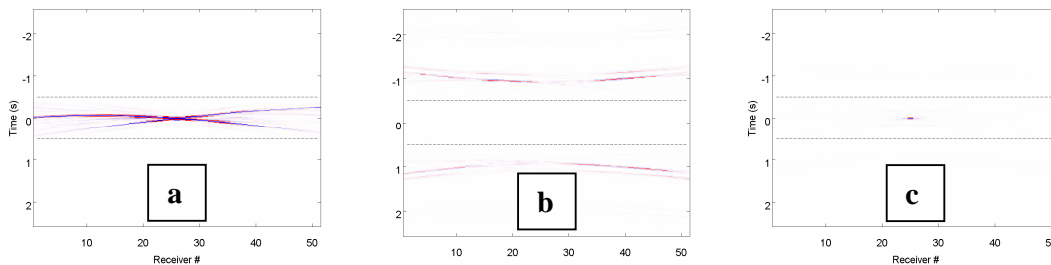


Figure 3: (a) Slice of $\hat{\mathbf{V}}_0\hat{\mathbf{V}}_0^\dagger$, (b) slice of $[\hat{\mathbf{V}}_s\hat{\mathbf{V}}_0^\dagger + \hat{\mathbf{V}}_0\hat{\mathbf{V}}_s^\dagger]$, (c) slice of $\hat{\mathbf{V}}_s\hat{\mathbf{V}}_s^\dagger$; all gathers have a similar amplitude scale and a virtual source at receiver 26; the maximum in (a) is clipped.

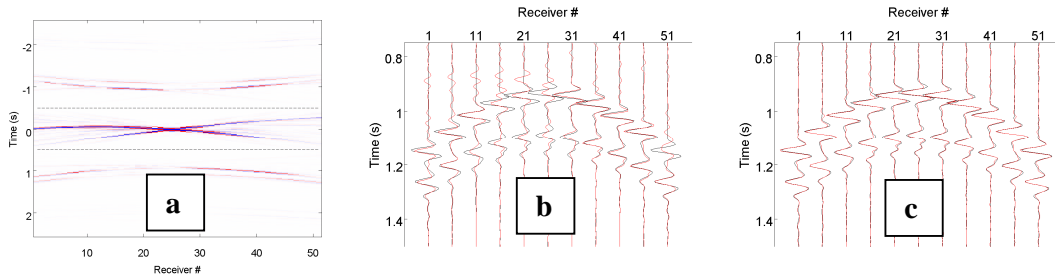


Figure 4: (a) Slice of $\hat{\mathbf{V}}^{\dagger}$ at virtual source 26; retrieved response by (b) cross-correlation and (c) multi-dimensional deconvolution (both in red) versus the reference response (in black) using time-gating after cross-correlation from transient sources and a virtual source at receiver 26.

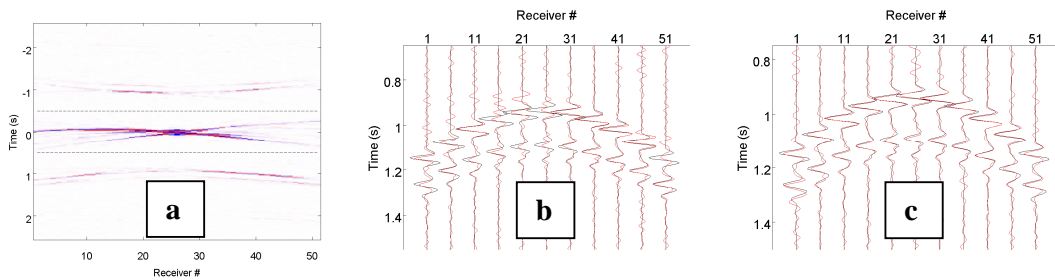


Figure 5: (a) Slice of $\langle \hat{\mathbf{V}}(A)\hat{\mathbf{V}}^*(A) \rangle$ at virtual source 26; retrieved response by (b) cross-correlation and (c) multi-dimensional deconvolution (both in red) versus the reference response (in black) using time-gating after cross-correlation from simultaneously acting noise sources and a virtual source at receiver 26.

Acknowledgements

This work is supported by The Netherlands Research Centre for Integrated Solid Earth Science (ISES); the Netherlands Organisation for Scientific Research (NWO, Toptalent 2006 AB); and the Dutch Technology Foundation (STW), an applied science division of NWO and the technology program of the Ministry of Economic Affairs (grant DCB.7913).

References

- Berkhout A.J., 1982. Seismic migration. Imaging of acoustic energy by wave field extrapolation. *Elsevier*.
- Draganov D., Campman X., Thorbecke J., Verdel A. and Wapenaar K., 2009, Reflection images from ambient seismic noise. *Geophysics*, **74**, A63-A67.
- Menke W., 1989. Geophysical data analysis. *Academic Press*, San Diego, CA.
- Van Groenestijn G.J.A. and Verschuur D.J., 2009, Estimation of primaries by sparse inversion from passive seismic data. 79th International Meeting Society of Exploration Geophysicists, expanded abstracts, 1597-1601.
- Wapenaar K. and Fokkema J., 2006. Green's function representations for seismic interferometry. *Geophysics*, **71**, SI33-SI46.
- Wapenaar K., Van der Neut J. and Ruigrok E., 2008. Passive seismic interferometry by multidimensional deconvolution. *Geophysics*, **73**, A51-A56.